A Study of The Deflagration-To-Detonation Transition and Its Limits of Hydrogen-Air Mixtures in An Open-Ended, Obstructed Channel

Henriksen, M., Pykhtina A., Gaathaug V.A., Vaagsaether K., Bjerketvedt D.
Faculty of Technology, Natural Sciences and Maritime Sciences, University of South-Eastern Norway, Kjølnes Ring 56, Porsgrunn, 3901, Norway

1 Introduction

The deflagration-to-detonation transition (DDT) process can occur if a flame is sufficiently accelerated, and with the right conditions, it can transition into a detonation wave [1–3]. This paper studies the DDT of hydrogen-air mixtures in a 1-meter highly obstructed open-ended channel at standard atmospheric pressure and temperature. The hydrogen flame will initially propagate approximately laminar but will become highly turbulent as it propagates through the obstructed part. As the flame leaves the obstructed zone of the channel, there is a probability for a DDT to occur. Several experiments were conducted to find the range of fuel-air equivalence ratios (ϕ) where DDT could happen. Additionally, two high-speed cameras with different imaging techniques were used to study the DDT process.

2 Methods and Materials

The experimental setup and procedure have been similarly described in previous studies [4–7]. The explosion channel's length, width, and height are 1000.0 mm, 65.0 mm, and 116.5 mm, respectively. In the explosion channel, there are 40 cylinders evenly placed approximately in the center of the channel. Each cylinder has a diameter of 18 mm and a length of 650 mm. Furthermore, the distance between the cells in the vertical and horizontal direction is 4.6 mm (±0.1 mm), creating a 0.5 void ratio and a maximum cross-section blockage ratio (BR) of 0.77 in the obstructed part of the channel. The first column of cells is 400 mm from the closed end of the channel. Figure 1 a) shows a photo of the explosion channel with the 40 cylinders and Fig. 1 b) shows a schematic illustration of the experimental setup with dimensions.

The premixed hydrogen-air inlet is located 50 mm from the closed end of the channel. With a porous lid attached to the open end of the channel, the channel's volume was exchanged eight times to ensure a homogenous mixture. Two Bronkhorst Mini-Cori-Flow Coriolis mass flow meter was used to set and record air and hydrogen mass flow during filling. After filling, there was a 20-second delay before ignition to reduce convective flow. Moreover, the ignition duration was 0.02 s, which gives two sparks generated from an AC transformer with an output voltage of 10 kV and a current of 20 mA. At the top of the channel, four Kistler pressure transducers spaced 250, 450, 650, and 850 mm from the closed end

Correspondence to: mathias.henriksen@usn.no

of the channel measure the explosion pressure. Three high-speed cameras were used to record the flame propagation. A Photron SA1 high-speed camera operating at 15 000 frames per second (fps) was used to record the self-luminescent flame propagation upstream from the cylinders. The Photron SAZ high-speed camera operating at 90 000 fps, recorded the self-luminescent flame propagation downstream from the cylinders. A focused shadowgraph setup was used at different locations downstream of the cylinders to capture the DDT phenomena. The Kirana high-speed camera used in the focused shadowgraph setup operated at 500 000 fps.

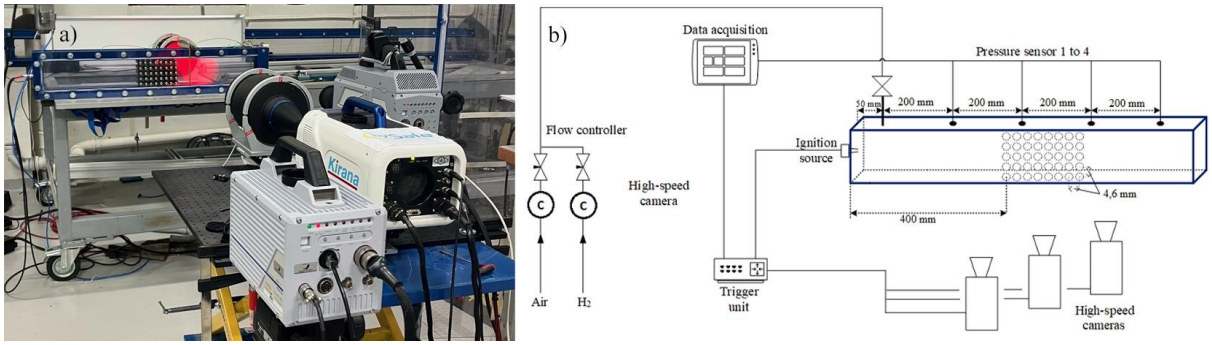

Figure 1: Photo and schematic illustration of the 1-meter explosion channel. a): Photo of explosion channel; b): Schematic illustration of the experimental setup with dimensions.

3 Results and Discussions

Table 1 shows the summarized experimental results. The lower and upper concentration limit, where DDT did not occur, was found at a ϕ of 0.9 and 1.5 (±0.02), respectively. DDT was mainly determined by analyzing the self-luminescent flame in the Photron SAZ high-speed images. This was because deflagration and DDT experiments could be challenging to distinguish from the recorded pressure alone. By contrast, the light emitted from the onset of DDT and the detonation wave were easily distinguished from that of a deflagration wave.

Table 1. Preliminary Experimental Results Summary

Number of Experiments	Fuel-Air Equivalence Ratio (±0.02)	Number of Experiments where DDT occurred	Probability of DDT
10	0.9	0	0
18	1.0	14	0.78
10	1.1	8	0.8
20[1]	1.2	10	0.5
5	1.3	1	0.2
5	1.4	1	0.2
10	1.5	0	0

[1] Experiments from Henriksen et al [7].

DDT limits in an open-ended channel with a single obstruction were studied by A.V. Gaathaug [8]. The study showed no DDT occurred for ϕ equal to 0.88, where the BRs were 0.9 or lower. Furthermore, the study found that DDT did occur for ϕ equal to 1.28 with a BR between 0.75 and 0.9, but not for ϕ equal to 1.59 and a BR of 0.6. Although the BR is lower and the ϕ higher in by A.V. Gaathaug study, the lower and upper limit of ϕ for DDT presented agrees reasonably well with the results shown in Table 1.

One important distinction between this study and A.V. Gaathaug's study [8] is the distance from the obstacle to the onset of DDT. In all experiments (except one) presented in A.V. Gaathaug's study, the onset of DDT occurred further downstream than in the current study. For 9 out of the 17 experiments where DDT occurred in [8], the distance from the obstacle to the onset of DDT is further than the length of the last section of the channel in this study. This indicates that cylinder geometry in this channel can significantly shorten the distance of onset of DDT.

Since parallel experiments did not always produce a DDT, the probability of DDT was included in Table 1. The highest likelihood of DDT was found at ϕ equal to 1.1 (±0.02). However, the experimental campaign and the scope of the paper were not to determine the probability of DDT; therefore, there is a lack of parallel experiments at some ϕ. The probability of DDT would likely increase if the length of the channel downstream of the cylinders were extended.

As mentioned, none of the ϕ gave a probability of 1 for DDT. In a previous study [7], 20 parallel experiments at ϕ equal to 1.2 were studied to see the possibility of and DDT process. The study showed that a hot spot needed to form slightly downstream from the cylinders for a DDT to occur. Similarly, in this study, a hot spot was seen in all experiments where DDT occurred. In the previous study, it was hypothesized that the collision of two transverse shocks formed the hot spot. However, the hypothesis could not be confirmed due to the imaging technique used. This study used a focused shadowgraph imaging technique downstream from the cylinders to analyze the flame propagation and shock waves in more detail. The flame propagation out of the cylinders. a): A series of high-speed images of self-illumination flame propagation. b): A series of shadowgram images of the flame propagation. Figure 2, Figure 3, and Figure 4 are series of shadowgram images and images of a self-luminescent flame, each figure representing different locations in the channel downstream from the cylinders.

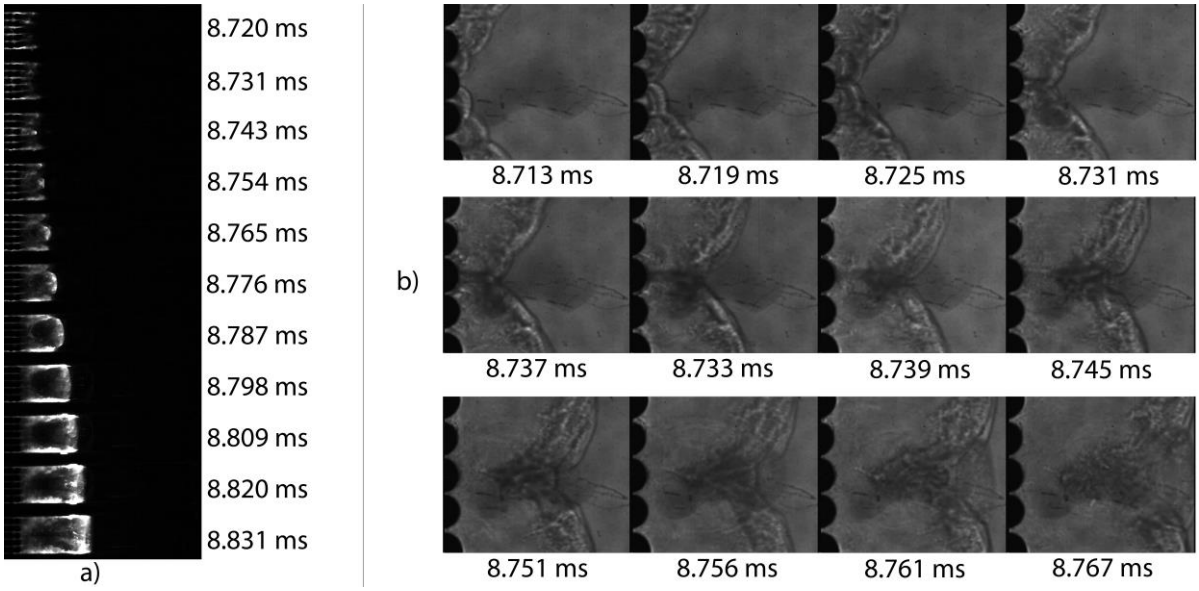

Figure 2. The flame propagation out of the cylinders. a): A series of high-speed images of self-illumination flame propagation. b): A series of shadowgram images of the flame propagation.

Figure 2 shows the flame as it leaves the cylinders. The hot spot formation could have been caused or aided by shock waves generated inside the geometry, which exits the cylinders ahead of the flame. However, no shock waves were seen leaving the cylinders before the flame. Moreover, as the flame exits the cylinders, it is impossible to distinguish the shock waves from the flame front in the shadowgram images. As the flame propagates downstream, the flame front and shock start to separate, as seen in the upper part of the shadowgrams at 8.733 ms and 8.739 ms. This suggests that the hot spot is formed due to shock collisions caused by a local explosion as the flame exits cylinders.

The formation of a hot spot is most easily seen first in the self-luminescent flame images in Figure 2 a) at 8.743 ms. It looks like the hot spot occurs a bit in front of the flame front at 8.743 ms in Figure 2 a); however, Figure 2 b) shows this is not the case. Although the hot spot's formation cannot be easily seen in Figure 2 b), it's clear that it occurs in the crest/elbow of the flame. From 8.751 ms to 8.767 ms in Figure 2 b), shows the evolution of the hot spot, which starts to propagate faster the upper shock wave in front of the initial flame. The onset of DDT is not seen in the shadowgrams in Figure 2 b), which occurs later at image 8.809 ms in Figure 2 a).

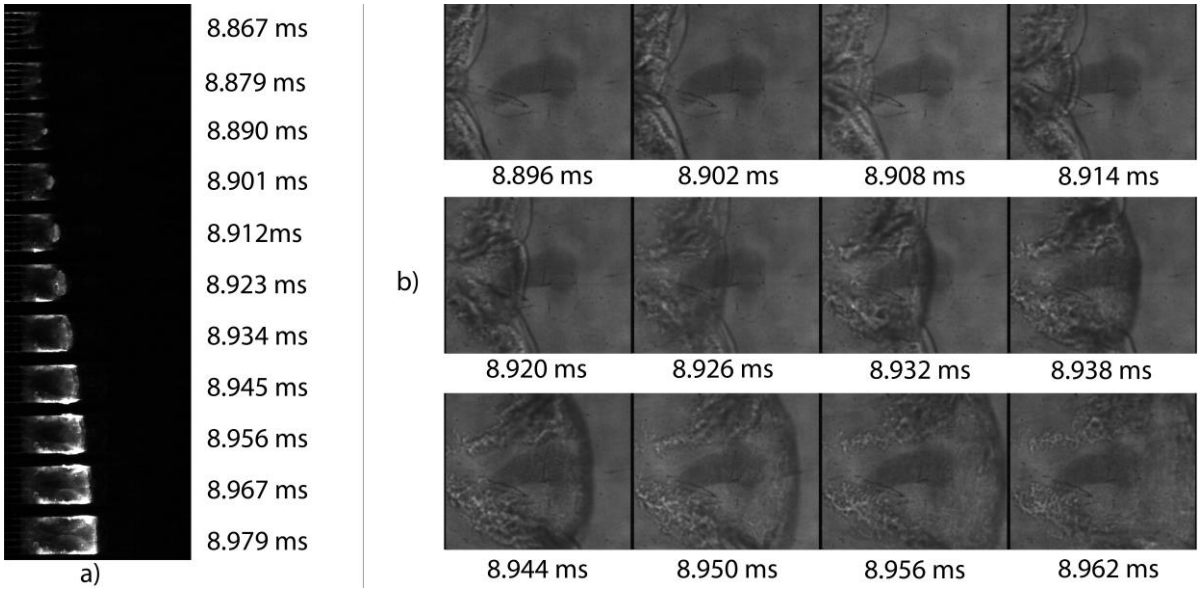

Figure 3. The flame propagation downstream of the cylinders; a) A series of high-speed images of a self-illumination flame propagation; b) A series of shadowgram images of the flame propagation.

In Figure 3 b), the shadowgraphy setup was moved slightly downstream from the position in Figure 2 b) to capture the evolution of the hot spot at the onset of DDT. Similar to the last shadowgrams in Figure 2 b), Figure 3 b) shows that the hot spot starts in the crest of the flame and propagates faster than the upper and lower shock in the channel. For the experiments with no hot spot, a clear separation of the flame front and shock wave was observed in the shadowgram images. When the new flame front formed by the hot spot reaches the walls of the channel, the onset of DDT occurs, as seen at 8.945 ms in Figure 3 a). Unfortunately, since the beginning of DDT occurs at the channel walls, which is not shown in the shadowgram images, it isn't easy to see the DDT in Figure 3 b)

Figure 4 a) shows the onset of the DDT process at 8.910 ms, which leads to the flat detonation front seen at 8.966 ms. Conversely, the transition is less easily seen in the shadowgram images in Figure 4 b). The shadowgram at 8.923 ms shows a transverse shock propagating from the bottom and up. The transvers shock is most likely due to the initiation of the DDT process. After the shock reaches the flame front at 8.935 ms, the front becomes sharper as the detonation wave front develops, as shown in the last three shadowgram images in Figure 4 b).

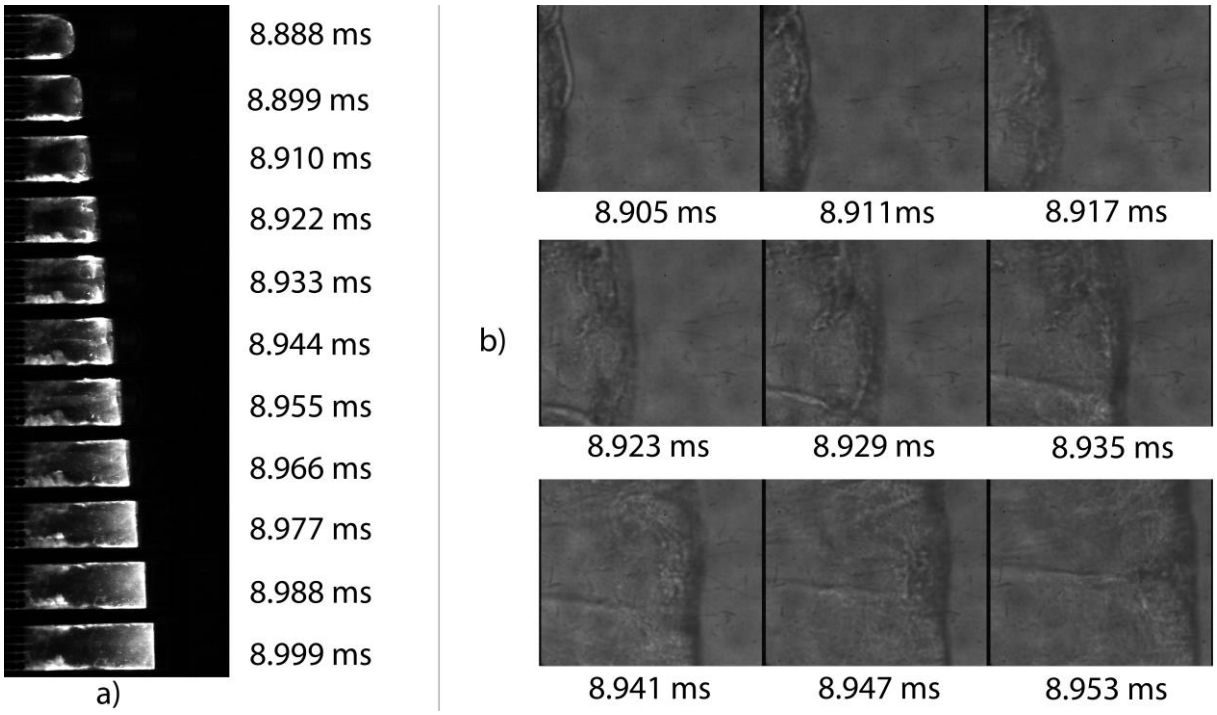

Figure 4. The flame propagation further downstream of the cylinders; a) A series of high-speed images of a self-illumination flame propagation; b) A series of shadowgram images of the flame propagation.

All the experiments where DDT occurred followed the processes described in the previous sections above and shown in Figure 2, Figure 3, and Figure 4. For DDT to occur in the proximity of the cylinders, a hot spot must be formed due to shock focusing slightly downstream from the cylinders. Although a hot spot is required for DDT in this channel, we have deliberately separated it from the DDT process since it is uncertain if the hot spot could sustain a DDT on its own. For the range of ϕ where DDT could occur, the flame propagation out of the cylinders had the same shape as seen in Figure 2 b) for DDT to occur. If flame propagation were more uneven at the top and bottom, DDT would not happen.

Conclusion

This study investigated the hydrogen-air ϕ limits of DDT at standard atmospheric conditions in a 1-meter-long obstructed channel by varying the ϕ. In addition, the DDT process is described in detail to understand the transition. The lower and upper ϕ limit for hydrogen, where DDT did not occur, was found to be 0.9 and 1.5 (±0.02), respectively. A similar lower DDT limit in an open-ended channel was found in a study by Andre Gaathaug [8].

In all the experiments where DDT occurred, an initial hot spot was needed to form slightly downstream from the cylinders. The hot spot was generated in the crest of the flame, most likely by shock wave collisions from the local explosion, which occurred when the flame exited the cylinder geometry. The shape of the flame as it left the geometry was essential for the hot spot formation. The onset of DDT happens when the flame front formed by the hot spot reaches the channel walls.

References

[1] Urtiew PA, Oppenheim AK. Experimental observations of the transition to detonation in an explosive gas. Proc R Soc Lond Ser Math Phys Sci 1966;295:13–28. https://doi.org/10.1098/rspa.1966.0223.
[2] Knystautas R, Lee JH, Moen I, Wagner HGg. Direct initiation of spherical detonation by a hot turbulent gas jet. Symp Int Combust 1979;17:1235–45. https://doi.org/10.1016/S0082-0784(79)80117-4.
[3] Lee JHS. Initiation of Gaseous Detonation 1977:30.
[4] Henriksen M, Vaagsaether K, Lundberg J, Forseth S, Bjerketvedt D. Simulation of a premixed explosion of gas vented during Li-ion battery failure. Fire Saf J 2021:103478. https://doi.org/10.1016/j.firesaf.2021.103478.
[5] Henriksen M. A study of premixed combustion of gas vented from failed Li-ion batteries. University of South-Eastern Norway, 2021.
[6] Henriksen M, Vaagsaether K, Lundberg J, Forseth S, Bjerketvedt D. Numerical study of premixed gas explosion in a 1-m channel partly filled with 18650 cell-like cylinders with experiments. J Loss Prev Process Ind 2022:15. https://doi.org/10.1016/j.jlp.2022.104761.
[7] Henriksen M, Vaagsaether K, Bjerketvedt D. Deflagration-to Detonation Transition of Hydrogen-Air Mixture in a Highly Congested, Open-ended Channel, Oslo, Norway: USN; 2022, p. 107–15.
[8] Gaathaug AV. Experimental Study of Deflagration to Detonation Transition in Hydrogen-Air Mixtures n.d.:191.